horticulturae

MDPI

Article

Translocation and Utilization Mechanisms of Leaf Intracellular Water in Karst Plants *Orychophragmus violaceus* (L.) O. E. Schulz and *Brassica napus* L.

Deke Xing [1], Weixu Wang [1], Yanyou Wu [2,*], Xiaojie Qin [1], Meiqing Li [1], Xiaole Chen [1] and Rui Yu [1]

[1] School of Agricultural Engineering, Jiangsu University, Zhenjiang 212013, China
[2] State Key Laboratory of Environmental Geochemistry, Institute of Geochemistry, Chinese Academy of Sciences, Guiyang 550081, China
* Correspondence: wuyanyou@mail.gyig.ac.cn; Tel.: +86-851-84391746

Abstract: *Orychophragmus violaceus* (L.) O. E. Schulz adapts to karst environments through a variety of adaptability mechanisms. However, the leaf intracellular water translocation and utilization mechanism is still unknown. This study hypothesizes that plants adapt to dehydration by synergistically adjusting the leaf anatomy, cell elasticity and intracellular water translocation. Leaf structure, elastic modulus (Em), physiological capacitance (CP), impedance (Z), water potential (Ψ_L), leaf tensity (LT) and chlorophyll fluorescence parameters of the detached leaves in plants of *O. violaceus* and *Brassica napus* L. were measured at each water loss time (0, 1, 2, 3, 4 and 5 h). The uniform leaves were randomly selected from five different plants for each species. The cell vacuole volume and translocation resistance of intracellular water could be represented by the electrophysiological parameters, such as CP and Z. The results indicated that timely shrinkage of *O. violaceus* leaves and mesophyll cells together with the increased water translocation resistance retained the intracellular water and maintained the turgor pressure. Water within sponge parenchyma could also be translocated into palisade parenchyma. The PSII reaction center was kept stable, and the photosynthetic activity of *O. violaceus* was clearly inhibited at 3 h. Palisade parenchyma of *B. napus* leaves increased quickly to improve the intercellular water translocation due to the strong cell stiffness. Gradually increasing intracellular water translocation resistance and recovery of the cell elasticity slowed down the leaf water loss, which, however, could not timely stop the damage on the PSII reaction center and the photochemical efficiency. The photochemical efficiency was seriously inhibited at 4 h and 5 h. The response mechanism of intracellular water to dehydration can be investigated with the help of leaf electrophysiological traits. However, the direct determination of plant drought resistance using electrophysiological information can still not be realized at present and needs further research.

Keywords: electrophysiology; anatomical structure; water potential; cell elasticity; water status

Citation: Xing, D.; Wang, W.; Wu, Y.; Qin, X.; Li, M.; Chen, X.; Yu, R. Translocation and Utilization Mechanisms of Leaf Intracellular Water in Karst Plants *Orychophragmus violaceus* (L.) O. E. Schulz and *Brassica napus* L. *Horticulturae* **2022**, *8*, 1082. https://doi.org/10.3390/horticulturae8111082

Academic Editors: Rossano Massai and Othmane Merah

Received: 5 September 2022
Accepted: 14 November 2022
Published: 16 November 2022

1. Introduction

The soils in karst areas are characterized by karst drought, high pH, low nutrients and high bicarbonate. Droughts with a high degree of spatial heterogeneity in these areas tend to occur increasingly frequently, which is the key factor limiting plant growth and deteriorating the fragile karst environment [1]. *Orychophragmus violaceus* (L.) O. E. Schulz belongs to Cruciferae, and is commonly called Chinese violet cress [2]. Some scholars strongly recommend this typical karst adaptable plant as a marginal raw material for terrestrial biomass [3]. This species is also cultivated as a medicine or ornamental plant and has wide market prospects. Cultivation of this plant helps to improve the economic income of local farmers in karst areas. *O. violaceus* is always taken as a model plant for studying the adaptive mechanisms of plants under karst adversities. It has been reported that *O. violaceus* adapts to karst adversities through a variety of adaptability mechanisms, i.e., photosynthetic adjusting, carbonic anhydrase regulation [4] and inorganic nutrient utilization [5].

Brassica napus L. is also a cruciferous plant with good karst drought resistance. *B. napus* is an important oil crop in southern China, as this type of crop can extract edible oil and fuel, thus having great economic value [6]. Besides, studies have reported that *O. violaceus* and *B. napus* are all suitable as pioneer plants for ecological restoration in karst areas, but they are different in adaptive mechanisms and drought resistance. Consequently, the *B. napus* plants were selected as a comparative species for conducting the investigations on the leaf intracellular water of *O. violaceus*. The studies on plant adaptive mechanisms aim to find methods for effectively evaluating plant stress resistance and matching the heterogeneous karst adversities during the ecological restoration. However, the determining methods established based on the above-mentioned adaptive mechanisms are time consuming and cannot determine the dynamic adaptability of a plant. In fact, plants adapt to adversities, especially drought stress, by the timely regulation of photosynthesis and growth, which is directly related to the intracellular water. Therefore, this study aims at investigating the translocation and utilization mechanisms of leaf intracellular water in karst adapted plants, and providing a basis for establishing a new method for effectively evaluating plant drought resistance in the short-term.

Water stress alters metabolisms in plants, thereby reducing photosynthesis and limiting plant growth [7]. Most (about 97%) of the water absorbed by plant roots dissipates through transpiration, but only a small amount (1~3%) is retained in leaf cells to support plant photosynthesis, growth and other physiological and biochemical processes. Researchers have measured the drought resistance of plants by abscisic acid and the indicators related to metabolism or osmoregulation. Abscisic acid (ABA) can induce stomatal closure and reduce water loss in plants under water deficit [8]. To avoid cell damage, plants produce substances such as phenolic compounds, proline, sugars, anthocyanins and glycosides, which have protective effects on osmoregulation [9]. The intracellular water required for photosynthesis is also regulated by carbonic anhydrase [10]. In fact, leaf intracellular water regulated by the above-mentioned strategies exhibits complex changes, which makes the determination of leaf intracellular water more difficult. Karst plants have made adaptive changes in the anatomical structure and cell behavior for surviving, which can be reflected by the leaf mechanical and electrophysiological traits. These leaf physical traits can be easily determined and are responsive.

Plant leaves are the most sensitive organs to adversities. Leaves can balance water gain and loss by rapidly adjusting anatomical structure and mechanical properties [11]. A water deficit can cause the leaf to shrink, and lead to changes in leaf density (LD) and water movement within leaves, which can reduce water loss [12]. High leaf water storage capacity is related to the increase in total leaf thickness, palisade tissue thickness, and spongy tissue thickness [13]. Leaf elastic modulus (Em) varies with LD and can reflect the variation of leaf anatomy. However, the leaf anatomical and mechanical properties only reflect the static water status of plant. Leaf water potential (Ψ_L) follows a circadian rhythm parallel to atmospheric evapotranspiration demand [14], and leaves can improve their absorption ability of water after a certain drop in Ψ_L. Water loss also induces mesophyll cells to generate and maintain a certain turgor pressure, thus changing the variation in Ψ_L [15]. Leaf electrophysiological information is increasingly used for detecting plant water status. A mesophyll cell can be modeled as a concentric sphere capacitor due to the special composition and structure [16]. A cell membrane with strictly selective permeability will influence the concentration of intracellular electrolytes. The water metabolism in leaves alters the electrolyte concentration and changes the corresponding electrophysiological parameters [12]. Intracellular water status can be obtained by measuring the electrophysiological indicators such as physiological capacitance (CP), impedance (Z) and leaf tensity (LT) of plant by a self-made parallel-plate capacitor [16]. Measurements of Ψ_L and electrophysiological information can investigate the dynamic leaf water status. It is apparent that the leaf intracellular water dynamic as well as the static status is of equal importance for regulating the water availability. However, the synergistic mechanism of leaf anatomy,

mechanical strength, Ψ_L and intracellular water translocation on intracellular water status has not been reported yet.

Leaf dehydration is easy to be controlled, so experiments can be repeated multiple times, data are more reliable and changes recorded during dehydration are not affected by other parts of the plant [17]. In this study, the detached leaves of *O. violaceus* and *B. napus* were used as experimental materials, they were soaked in double-distilled water for 30 min and then quickly dehydrated. By comparing the corresponding changes of chlorophyll fluorescence parameters such as maximum photosystem II (PSII) quantum efficiency (F_v/F_m), electron transport rate (ETR), photochemical quenching (qP) and non-photochemical quenching (NPQ) at different times of water loss, the photosynthetic characteristics of *O. violaceus* and *B. napus* were studied. The synergistic influence of leaf anatomical structure, mechanical strength, Ψ_L and intracellular water translocation on the water status were determined, and the photosynthetic adaptive mechanisms were investigated. This study hypothesized that plants can adapt to dehydration by synergistically adjusting the leaf anatomy, cell elasticity and intracellular water translocation. The results of this study can provide a new method for determining the leaf intracellular water and provide a basis for improving the evaluating efficiency of drought resistance of pioneer plants for ecological restoration in karst areas.

2. Materials and Methods

2.1. Plant Materials

The experiment was conducted in the lab at Jiangsu University, Jiangsu Province (32.20° N, 119.45° E), China. The leaves of *Orychophragmus violaceus* (L.) O. E. Schulz and *Brassica napus* L. were selected as the experimental materials in this study. The study area receives a mean annual air temperature of about 15.6 °C. The fourth and fifth fully expanded uniform leaves were completely randomly taken from five different plants for each species at 09:00–10:00 in the morning and immediately soaked into double-distilled water for 30 min, in order to make sure all the leaves were in a uniform initial state (water-saturated). As such, an accurate comparison could be made between *O. violaceus* and *B. napus*. Thereafter, the water on the leaf's surface was wiped off, and the leaves were placed on a dry and ventilated table (26 °C for 5 h). Next, the measurements were taken at 0 (baseline), 1, 2, 3, 4 and 5 h after dehydration, and the determination of each parameter was repeated five times with five different randomly selected leaves [10]. The photosynthetic photon flux density (PPFD) in the lab was 160 μmol/m^2·s, and the relative air humidity was 40 ± 5%.

2.2. Determination of Leaf Water Potential, Leaf Area and Water Content

Leaf water potential (Ψ_L) was determined by using a dew point microvoltmeter in a universal sample room (*C-52-SF, Psypro*, Wescor, Logan, UT, USA). The leaves were scanned with a broad-leafed image analysis system (*WinFOLIA, Regent Instruments Inc.*, Quebec, Canada) to obtain the leaf area (LA, cm^2). The fresh weight of the leaves (FW, g) was recorded. The leaves were then dried in an oven at 80 °C to constant weight (DW, g). The leaf water content (WC, %) was calculated by the following [18]:

$$WC = \frac{FW - DW}{FW} \times 100\% \quad (1)$$

2.3. Leaf Elastic Modulus Measurement

The increased stresses (F_s, N) with increasing deformation rates (ΔX, %) of leaf at each water loss time were recorded with the texture analyzer TA.XtplusC (Stable Micro Systems, Godalming, Surrey, UK) using the P/2n probe with a diameter of 2 mm. The working parameters and test mode were set up according to Xing et al. [10], and then the leaf elastic modulus (Em, N per unit of deformation) was calculated according to the following equation:

$$F_s = Em \times \Delta X \quad (2)$$

2.4. Determination of Leaf Anatomy and Leaf Density

Leaf anatomy was observed by using the paraffin sectioning method [19]. Leaf pieces (0.5 × 0.5 cm) were cut off between the main veins and immersed under the formalin-acetic acid-alcohol (FAA) fixing solution [10]. These paraffin sections were stained with safranin and fast green dye and permanently mounted on slides. Samples were observed by using inverted light microscopes (DMi8, Leica, Wetzlar, Germany), and images were taken. The leaf's total thickness (D_t, μm), upper and lower epidermis thickness, palisade parenchyma thickness, sponge parenchyma thickness and palisade-sponge ratio (%) were measured by the ImageJ software (National Institutes of Health—NIH, Bethesda, MD, USA). The tightness degree of leaf tissue structure (CTR, %) is the ratio of palisade parenchyma thickness to leaf thickness, and loose degree of leaf tissue structure (SR, %) is the ratio of sponge parenchyma thickness to leaf thickness.

Leaf density (LD, g/cm^3) was calculated as follows:

$$LD = \frac{DW}{D_t \times LA} \times 10^4 \quad (3)$$

where DW (g) is the leaf dry weight, D_t (μm) is the leaf total thickness and LA (cm^2) is the leaf area.

2.5. Determination of Physiological Capacitance, Impedance and Leaf Tensity

The physiological capacitance (CP, pF) and impedance (Z, MΩ) at each water loss time was determined by using the LCR HiTester (model 3532-50, Hioki, Nagano, Japan) with a frequency and voltage of 3 kHz and 1 V, respectively [20]. Each leaf was clipped onto the custom-made parallel-plate capacitor. The value of LT (cm^2/cm) was calculated according to the following equation [21]:

$$LT = \frac{A_{CP}}{d_L} = \frac{CP}{\varepsilon_0}\left[\frac{1000iRT}{81,000iRT + (81 - a)M\Psi_L}\right] \quad (4)$$

where A_{CP} (cm^2) is the effective area of the leaf in contact with the capacitor plates, d_L (cm) is the leaf effective thickness, ε_0 is the vacuum dielectric constant (with value of 8.854 × 10^{-12} F/m); I is the dissociation coefficient (with value of 1), R is the gas constant (with value of 8.30 × 10^{-3} L·MPa/mol·K), T is the thermodynamic temperature (T = 273 + t °C, K), 81 is the relative dielectric constant of water at normal temperature, a is the relative dielectric constant of the cytosol solute, M is the relative molecular mass of the cytosol solute (g/mol), and Ψ_L (MPa) is the leaf water potential. In this study, the sucrose $C_{12}H_{22}O_{11}$ was identified as the solute in the cytosol, therefore, a was 3.30, M was 342 g/mol, and t was 20 °C [10].

2.6. Chlorophyll Fluorescence Parameters Measurement

Chlorophyll fluorescence (ChlF) parameters were determined by using an IMAGING-PAM modulated chlorophyll fluorescence imaging system (PAM-2000, Walz, Germany). Leaves were dark adapted for 30 min to ensure complete relaxation of all reaction centers before the measurements. The minimum fluorescence (F_o) was determined using a measuring beam, whereas the maximum ChlF (F_m) was recorded after a 0.8 s saturating light pulse (6000 μmol/m^2·s). Maximum PSII quantum yield (F_v/F_m) was calculated as ($F_m - F_o$)/Fm. Then the action light was applied, the minimum (F_o') and maximum (F_m') fluorescence under light and the steady state fluorescence (F_s) were recorded after the fluorescence value was stable. The electron transport rate (ETR) is calculated as follows: ETR = PPFD × Φ_{PSII} × 0.85 × 0.5, where the 0.5 represents the two-quantum absorption per electron transport, and 0.85 represents the absorbed part of the incident photon is 85%, PPFD is the photosynthetic photon flux density. The qP is calculated as follows: $qP = \frac{F_m' - F_s}{F_m' - F_o'}$, and the NPQ is calculated as follows: $NPQ = \frac{F_m - F_m'}{F_m'}$.

2.7. Statistical Analysis

Data are presented as means of at least five replicates (five uniform leaves from five randomly selected plants for each species). The results were analyzed by one-way ANOVA with the Duncan's multiple comparison at $p \leq 0.05$ with the SPSS22.0 software (*SPSS, IBM, Armonk,* New York, NY, USA). The statistically significant differences between different treatments for each species were determined, respectively. The data are shown as the means ± SE (n = 5).

3. Results

3.1. Leaf Water Potential, Leaf Area and Water Content

For O. violaceus, Ψ_L at 5 h was significantly lower than that at 0 h and 1 h, but there was no significant difference between the values at 2~5 h. LA decreased significantly with the increase of water loss time. The WC at 5 h was significantly lower than that at 0~3 h, but there was no significant difference between the values at 5 h and 4 h. For B. napus, Ψ_L and WC did not decrease significantly during the water loss, but the LA at 5 h was significantly lower than that at 0 h and 1 h (Table 1).

Table 1. Leaf water potential (Ψ_L, MPa), leaf area (LA, cm^2) and leaf water content (WC, %) at different dehydration times.

Species	Water Loss Time (h)	Leaf Water Potential	Leaf Area	Leaf Water Content
O. violaceus	0	−0.81 ± 0.05 a	20.10 ± 0.24 a	86.01 ± 1.20 a
	1	−1.12 ± 0.11 ab	19.31 ± 0.14 b	82.74 ± 0.95 b
	2	−1.20 ± 0.15 bc	18.77 ± 0.19 c	81.32 ± 0.82 bc
	3	−1.29 ± 0.14 bc	18.13 ± 0.12 d	79.05 ± 1.03 cd
	4	−1.49 ± 0.13 bc	17.45 ± 0.06 e	77.12 ± 0.96 de
	5	−1.58 ± 0.13 c	16.81 ± 0.02 f	75.75 ± 0.55 e
B. napus	0	−0.83 ± 0.08 a	22.97 ± 0.38 a	81.52 ± 1.35 a
	1	−1.00 ± 0.08 ab	22.68 ± 0.36 ab	79.94 ± 1.02 ab
	2	−1.02 ± 0.09 ab	22.39 ± 0.34 abc	79.10 ± 0.81 ab
	3	−1.10 ± 0.10 ab	21.98 ± 0.29 abc	78.49 ± 0.63 b
	4	−1.02 ± 0.08 ab	21.66 ± 0.30 bc	77.87 ± 0.60 b
	5	−1.20 ± 0.11 b	21.38 ± 0.29 c	77.11 ± 0.32 b

Note: Means (n = 5) in the same column for each plant species followed by different letters differ significantly at $p \leq 0.05$, according to one-way ANOVA.

3.2. Changes of Elastic Modulus and Leaf Anatomical Structure

The Em values of *O. violaceus* at 0, 1 and 3 h were significantly lower than those at other levels. There was no significant difference between the values at 2 h and 5 h (Figure 1A). The values of Em of *B. napus* at 0, 2 and 3 h were remarkably lower than that at 1 h but higher than that at 4 h, there was no significant difference between the values at 4 h and 5 h (Figure 1B).

With the extension of dehydration time, the values of total leaf thickness, sponge parenchyma and lower epidermis of *O. violaceus* at 3~5 h were significantly lower than those at 0 and 1 h, respectively. Additionally, the values of each parameter at 3~5 h exhibited no clear difference. The value of the upper epidermis at 4 h was clearly lower than those at 0~2 h, and the value of palisade parenchyma at 0 h was clearly higher than those at 1, 3 and 4 h (Table 2).

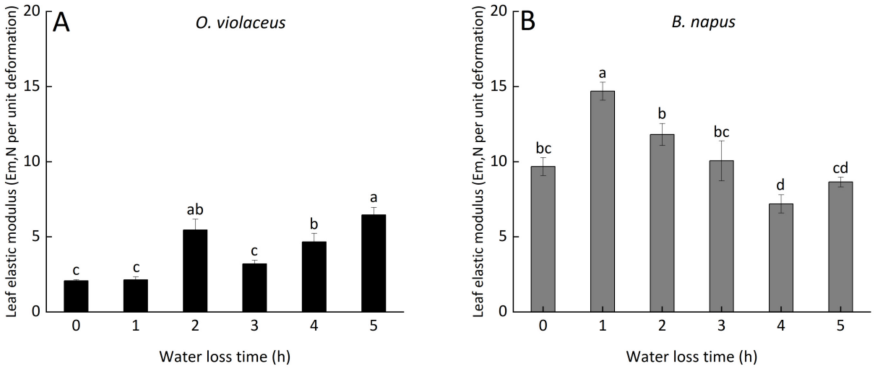

Figure 1. Changes of elastic modulus (Em, N per unit deformation) of *O. violaceus* (**A**) and *B. napus* (**B**). (Note: Different letters appear above the error bars of the same plant species when subsequent values differ significantly at $p \leq 0.05$, according to one-way ANOVA).

Table 2. Leaf anatomical parameters of *O. violaceus*.

Water Loss Time (h)	Thickness (μm)				
	Total Leaf Thickness	Upper Epidermis	Palisade Parenchyma	Sponge Parenchyma	Lower Epidermis
0	150.63 ± 7.57 a	13.97 ± 0.81 a	27.66 ± 1.69 a	95.02 ± 5.70 a	13.98 ± 0.69 a
1	142.42 ± 0.54 ab	13.15 ± 0.38 a	20.88 ± 2.80 b	94.54 ± 2.05 a	13.85 ± 0.04 a
2	130.18 ± 2.56 b	13.20 ± 1.17 a	26.13 ± 1.36 ab	79.71 ± 2.80 b	11.15 ± 0.46 b
3	100.59 ± 5.61 c	12.06 ± 0.62 ab	20.77 ± 1.30 b	57.87 ± 3.03 c	9.90 ± 0.73 bc
4	98.42 ± 3.85 c	10.09 ± 0.56 b	20.28 ± 1.09 b	58.62 ± 3.11 c	9.44 ± 0.24 bc
5	106.20 ± 2.49 c	11.93 ± 0.63 ab	23.93 ± 2.12 ab	61.59 ± 2.22 c	8.74 ± 0.67 c

Note: Means (n = 5) in the same column followed by different letters differ significantly at $p \leq 0.05$, according to one-way ANOVA.

Table 3. Leaf anatomical parameters of *B. napus*.

Water Loss Time (h)	Thickness (μm)				
	Total Leaf Thickness	Upper Epidermis	Palisade Parenchyma	Sponge Parenchyma	Lower Epidermis
0	154.41 ± 2.94 ab	17.09 ± 0.85 a	33.19 ± 0.47 c	95.59 ± 2.96 a	8.54 ± 0.33 b
1	155.90 ± 1.59 ab	16.95 ± 0.43 a	37.71 ± 1.03 b	90.55 ± 1.42 a	10.69 ± 0.85 a
2	157.80 ± 3.89 a	16.53 ± 0.88 a	40.54 ± 0.74 a	89.05 ± 3.85 a	11.68 ± 0.52 a
3	138.78 ± 2.27 c	15.67 ± 0.62 a	30.80 ± 0.79 cd	80.61 ± 1.01 b	11.70 ± 0.74 a
4	153.46 ± 4.17 ab	15.32 ± 0.31 ab	32.12 ± 0.73 c	94.90 ± 3.31 a	11.13 ± 0.38 a
5	146.88 ± 1.29 bc	13.59 ± 0.46 b	29.04 ± 0.64 d	94.32 ± 1.96 a	9.93 ± 0.76 ab

Note: Means (n = 5) in the same column followed by different letters differ significantly at $p \leq 0.05$, according to one-way ANOVA.

For *O. violaceus*, the palisade-sponge ratio at 1 h was significantly lower than those at 2~5 h, but showed no clear difference with that at 0 h. The CTR at 1 h was significantly lower than those at other water loss times, but there was no clear difference between those values at 2~5 h. The SR at 1 h was remarkably higher than those at 2~5 h, but had no significant difference with that at 0 h. For *B. napus*, the palisade-sponge ratio at 2 h was significantly higher than those at 0 h and 3~5 h, but showed no significant difference with that at 1 h, there was no significant difference between the values at 0, 4 and 5 h. The CTR values at 1 h and 2 h were significantly higher than those at other levels, but there was no significant difference between the values at 4 h and 5 h. The SR values at 1~3 h were significantly lower than those at 0, 4 and 5 h (Table 4).

Table 4. Comparison of leaf tissue characteristics between *O. violaceus* and *B. napus*.

Species	Water Loss Time (h)	Palisade-Sponge Ratio (%)	CTR (%)	SR (%)
O. violaceus	0	29.14 ± 1.05 bc	18.35 ± 0.40 b	63.04 ± 1.09 ab
	1	22.24 ± 3.49 c	14.65 ± 1.92 c	66.39 ± 1.62 a
	2	32.85 ± 2.07 ab	20.05 ± 0.74 ab	61.23 ± 1.76 bc
	3	35.86 ± 0.76 ab	20.63 ± 0.32 ab	57.55 ± 0.35 c
	4	34.70 ± 1.85 ab	20.60 ± 0.72 ab	59.50 ± 1.25 bc
	5	39.09 ± 4.26 a	22.52 ± 1.75 a	58.01 ± 1.85 c
B. napus	0	34.76 ± 0.74 cd	21.50 ± 0.19 b	61.88 ± 0.79 a
	1	41.69 ± 1.64 ab	24.19 ± 0.63 a	58.09 ± 0.83 b
	2	45.74 ± 2.53 a	25.73 ± 0.90 a	56.38 ± 1.14 b
	3	38.20 ± 0.51 bc	22.19 ± 0.21 b	58.09 ± 0.29 b
	4	33.88 ± 0.41 cd	20.94 ± 0.11 bc	61.81 ± 0.48 a
	5	30.83 ± 1.12 d	19.77 ± 0.49 c	64.20 ± 0.83 a

Note: Means (n = 5) in the same column for each plant species followed by different letters differ significantly at $p \leq 0.05$, according to one-way ANOVA.

3.3. Changes of Physiological Capacitance and Impedance

The electrophysiological parameters CP and Z could represent the cell vacuole volume and resistance of intracellular water translocation [21,22]. The values of CP of *O. violaceus* at 1, 5 h were lower than that at 0 h but higher than those at 3, 4 h (Table 5). The CP of *O. violaceus* at 4 h was lower than those at other levels. The Z value of *O. violaceus* at 4 h was clearly higher than those at 0~2 h and 5 h, those at 1, 2 and 3 h showed no clear difference and were higher than the values at 0 and 5 h. The CP value of *B. napus* at 1 h was significantly higher than those at other levels, and the value at 5 h was clearly lower than those at other levels, and there was no clear difference between the values at 3 h and 4 h. The CP of *B. napus* at 2 h was higher than that at 3 h or 4 h but lower than that at 0 h. The Z value of *B. napus* at 5 h was higher than those at other levels, but the values at 0 h and 1 h were clearly lower than those at 2, 4 and 5 h, and the value at 4 h was remarkably higher than those at 0~3 h (Table 5).

Table 5. Leaf physiological capacitance (CP, pF) and impedance (Z, MΩ) at different dehydration times.

Species	Water Loss Time (h)	Physiological Capacitance	Physiological Impedance
O. violaceus	0	165.829 ± 3.203 a	0.686 ± 0.026 c
	1	106.725 ± 0.112 bc	1.131 ± 0.088 b
	2	95.636 ± 0.694 cd	1.256 ± 0.049 b
	3	87.890 ± 7.766 d	1.328 ±0.092 ab
	4	65.463 ± 4.508 e	1.486 ± 0.086 a
	5	114.747 ± 3.202 b	0.875 ± 0.052 c
B. napus	0	278.716 ± 10.921 b	0.526 ± 0.027 de
	1	322.141 ± 10.274 a	0.412 ± 0.019 e
	2	161.440 ± 11.663 c	0.711 ± 0.032 c
	3	133.522 ± 3.965 d	0.641 ± 0.024 cd
	4	130.789 ± 1.907 d	1.017 ± 0.060 b
	5	99.254 ± 2.585 e	1.165 ± 0.082 a

Note: Means (n = 5) in the same column for each plant species followed by different letters differ significantly at $p \leq 0.05$, according to one-way ANOVA.

3.4. Changes of Leaf Tensity and Leaf Density

The LT values of *O. violaceus* at 1 and 2 h showed no significant difference, the value at 5 h was higher than those at 1~4 h but lower than that at 0 h. The LT of *O. violaceus* at 4 h

was clearly lower than those at other levels (Figure 2A). The LT value of *B. napus* at 0 h was higher than those at 2~5 h but lower than that at 1 h, the value at 5 h was significantly lower than those at other levels (Figure 2B). The LD values of *O. violaceus* increased significantly at 3, 4, and 5 h compared to those at 0, 1 and 2 h, there was no significant difference between the values at 3, 4 and 5 h (Figure 2C). The LD values of *B. napus* had no significant change at 0~2 h. The LD value of *B. napus* at 3 h was clearly higher than those at 0~2 h and 4 h (Figure 2D).

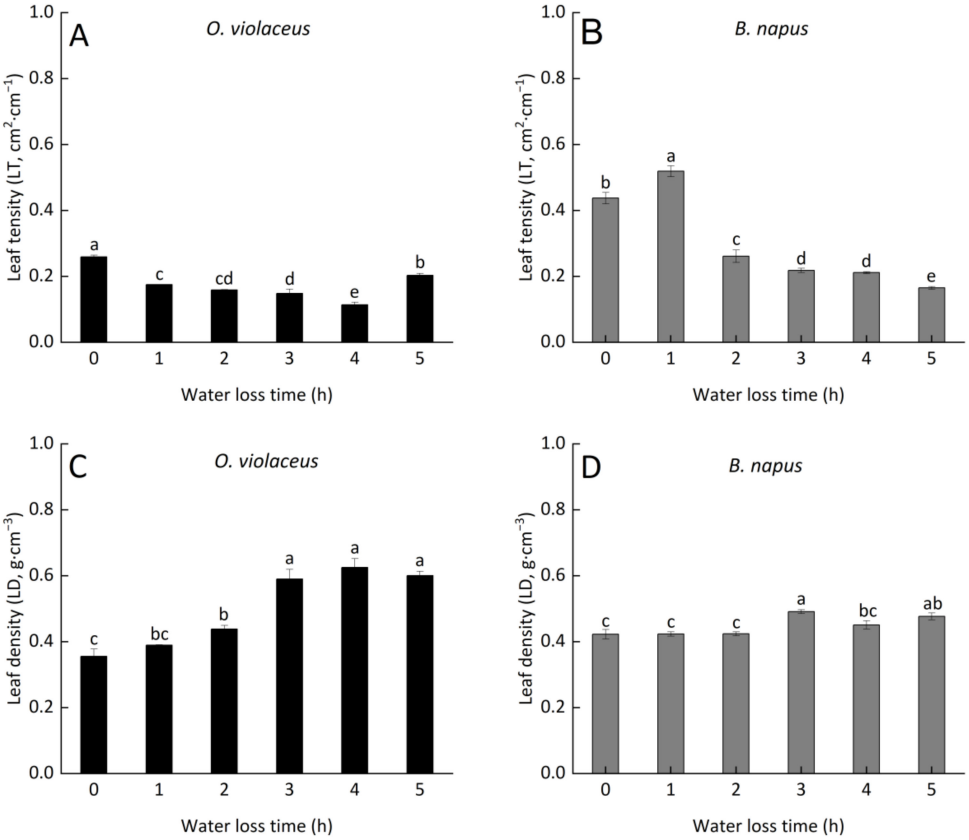

Figure 2. Leaf tensity (LT, $cm^2 \cdot cm^{-1}$) and leaf density (LD, $g \cdot cm^{-3}$) of *O. violaceus* and *B. napus* at different dehydration times. (Note: (**A**) LT of *O. violaceus*; (**B**) LT of *B. napus*; (**C**) LD of *O. violaceus*; (**D**) LD of *B. napus*. Different letters appear above the error bars of the same parameter in the same plant species when subsequent values differ significantly at $p \leq 0.05$, according to one-way ANOVA).

3.5. Chlorophyll Fluorescence Parameters

The F_v/F_m values of *O. violaceus* did not change significantly at 0~2 h, then decreased as dehydration time increased (Figure 3A). Lower F_v/F_m value of *B. napus* was associated with increasing dehydration time (Figure 3B). The ETR values of *O. violaceus* showed no clear difference at 1 and 2 h, and the values of *O. violaceus* at 3 and 4 h also showed no remarkable difference but were lower than those at 1 and 2 h. The ETR of *O. violaceus* at 0 h was remarkably higher than those at other levels, while that at 5 h was lower than the values at other levels (Figure 3C). The ETR values of *B. napus* kept stable at 2~4 h, which were clearly lower than that at 0 h but higher than that at 5 h (Figure 3D). The qP of *O. violaceus* at 3 h was higher than that at 1 h but lower than those at 0 and 2 h, and the values at 0 h and 2 h were significantly higher than those at other levels. The qP of *O. violaceus* at 5 h was clearly lower than those at other levels (Figure 3E). The qP of *B. napus* at 1~3 h showed no clear difference, they were significantly lower than the value at 0 h but higher than those at 4 h and 5 h (Figure 3F). The NPQ of *O. violaceus* increased remarkably at 1 h compared to that at 0 h, then exhibited no clear difference between the values at 1~4 h, the value at 5 h was significantly higher than those at 0~3 h, but showed no significant

difference with that at 4 h (Figure 3G). The NPQ values of *B. napus* at 4 h and 5 h were significantly higher than those at 0~2 h, but showed no significant difference with that at 3 h, and that at 0 h was clearly lower than the values at 2~5 h (Figure 3H).

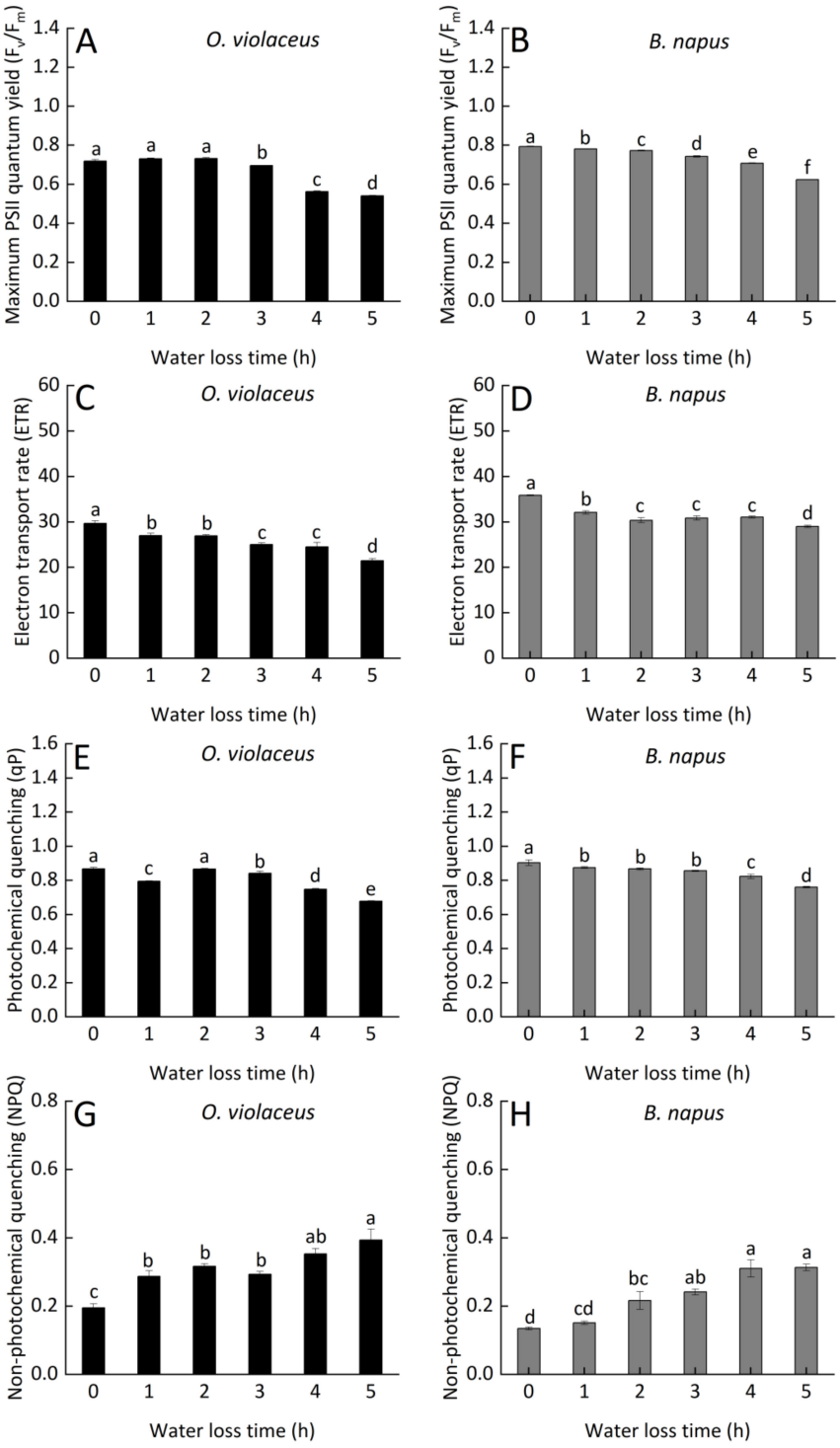

Figure 3. The F_v/F_m, ETR, qP and NPQ of *O. violaceus* and *B. napus* at different dehydration times (Note: (**A**,**C**,**E**,**G**) are the F_v/F_m, ETR, qP, NPQ of *O. violaceus*, respectively; (**B**,**D**,**F**,**H**) are the F_v/F_m, ETR, qP, NPQ of *B. napus*, respectively. Different letters appear above the error bars of the same parameter in the same plant species when subsequent values differ significantly at $p \leq 0.05$, according to one-way ANOVA).

4. Discussion

4.1. Leaf Intracellular Water Translocation vs. Anatomical Structure and Electrophysiology

The present study aimed to investigate the responses of leaf anatomical and physical traits of *O. violaceus* and *B. napus* to dehydration. Changes of palisade or spongy parenchyma in *O. violaceus* at different water loss times altered the intracellular water distribution. Water in spongy parenchyma of *O. violaceus* maintained stable at 1 h but was obviously lost at 3 h, while the water in palisade parenchyma maintained stable at 1~5 h (Figure 4). Most importantly, the electrophysiological indices, i.e., CP, Z, have been successfully used to determine the dynamic traits and metabolism of the intracellular water [16]. CP is closely related to the change of vacuole volume [21]. By analyzing variations of CP and Z of *O. violaceus*, we found that water translocation occurred within mesophyll cell or between palisade and spongy parenchyma at 1~5 h. Water was mainly translocated from spongy parenchyma into palisade parenchyma of *O. violaceus* at 3 h. Spongy parenchyma of *B. napus* shrank at 1~3 h and recovered at 5 h (Figure 4), the water was mainly translocated from spongy parenchyma into palisade parenchyma at 1~3 h, and the resistance of water translocation increased with increasing water loss times. *B. napus* leaf also exhibited lower water loss rate than *O. violaceus* during the dehydration period.

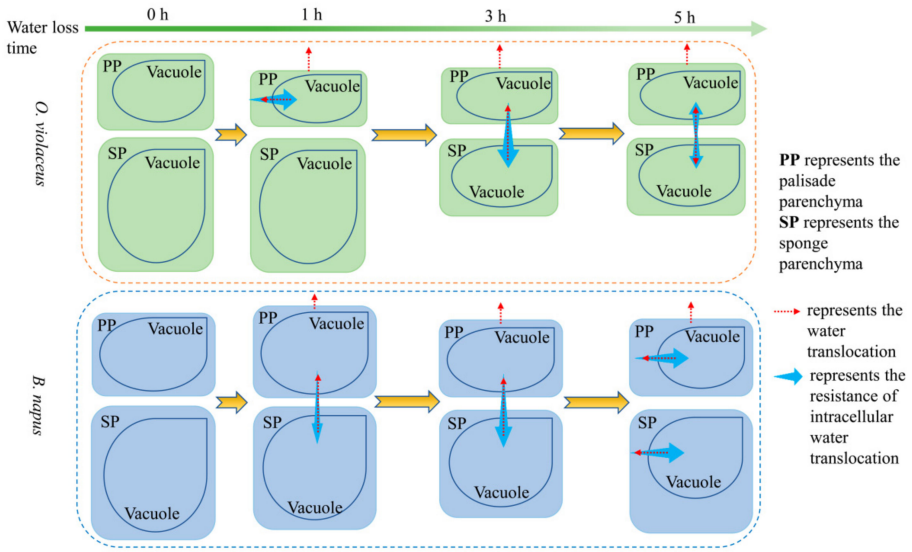

Figure 4. Leaf intracellular water translocation in *O. violaceus* and *B. napus*.

Anatomical structure, WC could just reflect the static leaf water status in a moment, and the determination of anatomical structure was destructive. However, plant electrophysiology determination was non-destructive and could be used to investigate the dynamic traits of intracellular water, which helped to study the water metabolism [23]. Therefore, it has the potential to quickly determine the dynamic adaptability of *O. violaceus* and *B. napus*.

4.2. Dynamic Leaf Water Status under Dehydration

Responses of leaf traits to dehydration differ between *O. violaceus* and *B. napus* but are all aimed at adjusting the leaf intracellular water and coping with water deficit environments [24]. At 1 h, spongy parenchyma contributed to the improvement of gas exchange [25], which kept the transpiration and water loss in *O. violaceus*. Due to the elasticity of mesophyll cells of *O. violaceus*, the palisade parenchyma was prone to shrink as further water losing [26], which, however, maintained the intracellular turgor pressure and kept the Ψ_L. Leaf Z represents the resistance to current, which is generated by the transport of dielectric materials including inorganic and organic ions. It is negatively correlated with the intracellular water transport rate [22]. Increased Z at 1 h enhanced the translocation resistance of intracellular water and maintained the intracellular substances.

Water loss at 1 h decreased the electron transport and photochemical efficiency, but did not affect the integrity of the PSII reaction center of *O. violaceus*. Mesophyll cells of *B. napus* with high stiffness helped to keep the leaf morphology and intracellular water. Increased palisade parenchyma might be attributed to the translated water from intracellular HCO_3^-, which was regulated by carbonic anhydrase in *B. napus* leaves [27]. Increased palisade parenchyma can improve the intercellular water transport efficiency and increase the mesophyll cell superficial area, therefore improving the leaf water holding capacity [28]. As a result, the intracellular water translocation resistance of *B. napus* was slightly reduced. However, PSII of *B. napus* was more sensitive to dehydration than *O. violaceus*.

At 2~3 h, mesophyll cells of *O. violaceus* with high elasticity were prone to shrink, caused by the increasing water loss. Sponge parenchyma occupies more spaces than palisade parenchyma in leaves [29]. Shrinking sponge parenchyma in *O. violaceus* leaves clearly decreased the mesophyll cell volume and reduced the transpired dissipation [25]. Meanwhile, water within the sponge parenchyma was translocated into palisade parenchyma, but the stable translocation resistance of intracellular water, which was kept by the increased CTR and slightly decreased Ψ_L, mitigated the water loss and maintained the leaf water status of *O. violaceus*. However, damage of dehydration on the PSII reaction center of *O. violaceus* became obvious at 3 h. No obvious water loss was observed due to the increased translocation resistance of intracellular water in *B. napus*. However, recovery of the cell elasticity of *B. napus* caused decrease in mesophyll cell volume but remarkably increased the LD and also maintained the Ψ_L. Meanwhile, the decreased CTR was conducive to the water movement among intercellular spaces. As a result, although the PSII reaction center of *B. napus* suffered from the damage, it could still maintain stable light transport and photochemical efficiency.

At 4~5 h, the mesophyll cells were prone to perform stiffness, and there was no obvious change in leaf anatomy of *O. violaceus*. The intra- and inter-cellular water movement declined due to the less WC and high LD, which alleviated the leaf water loss, kept the Ψ_L and reduced the translocation resistance of intracellular water. The latter one might also be attributed to the water regulation caused by carbonic anhydrase in *O. violaceus* leaves, since the carbonic anhydrase of *O. violaceus* would be activated under water deficit conditions [4]. However, water deficit at this period significantly inhibited the photochemical efficiency and damaged the PSII reaction center of *O. violaceus*. Previous studies have shown that the destruction of plant leaf epidermis leads to the reduction of photosynthesis and increase of water loss [30]. The upper epidermis of *B. napus* is thicker than that of *O. violaceus*, so it can prevent further water loss from leaves and kept the Ψ_L. The remaining intracellular water and cell elasticity recovered the volume of sponge parenchyma. The clearly increased intracellular water translocation resistance of *B. napus* indicated that the water movement within cells occurred. The photochemical efficiency was influenced by dehydration and was seriously inhibited at 4–5 h, which was attributed to the slow water loss in *B. napus* leaves.

5. Conclusions

This study explained the different translocation and utilization mechanisms of leaf intracellular water in *O. violaceus* and *B. napus* by analyzing the leaf anatomical and physical traits. Rapid water loss led to the timely shrinkage of *O. violaceus* leaves and mesophyll cells due to the better cell elasticity compared with *B. napus*, and the increased intracellular water translocation resistance helped to retain the intracellular water and maintain the turgor pressure. The water within the sponge parenchyma could also be translocated into the palisade parenchyma. Consequently, the PSII reaction center and photochemical efficiency were kept stable. Photosynthetic activity of *O. violaceus* was clearly inhibited after three hours from the onset of dehydration. Palisade parenchyma in *B. napus* leaves increased quickly to improve the intercellular water translocation due to the strong cell stiffness. Gradually increasing intracellular water translocation resistance, and the recovery of cell elasticity and thick upper epidermis, helped to slow down the leaf water loss, which,

however, could not timely stop the damage on the PSII reaction center and photochemical efficiency. The photochemical efficiency was influenced by dehydration and was seriously inhibited until 4 and 5 h, which was attributed by the slow water loss in *B. napus* leaves. The response mechanism of intracellular water to dehydration can be investigated with the help of leaf electrophysiological traits, thereby providing a basis for improving the evaluating efficiency of plant drought resistance. However, the rapid and direct determination of plant drought resistance by using leaf electrophysiological information can still not be realized at present and needs further research.

Author Contributions: Conceptualization, D.X. and Y.W.; methodology, W.W., D.X. and Y.W.; validation, X.C.; resources, X.Q. and R.Y.; data curation, W.W. and X.C.; writing—original draft preparation, W.W.; writing—review and editing, D.X. and M.L.; funding acquisition, Y.W. All authors have read and agreed to the published version of the manuscript.

Funding: This research was funded by the Support Plan Projects of Science and Technology of Guizhou Province [No. (2021) YB453], the National Key Research and Development Program of China [No. 2021YFD1100300], the Priority Academic Program Development (PAPD) of Jiangsu Higher Education Institutions, and the Graduate Innovative Projects of Jiangsu Province [2014(KYLX_1061)].

Institutional Review Board Statement: Not applicable.

Informed Consent Statement: Not applicable.

Data Availability Statement: The datasets during or analyzed during the current study are available from the corresponding author upon reasonable request.

Conflicts of Interest: The authors declare no conflict of interest.

References

1. Wu, Y.Y.; Xing, D.K.; Hang, H.T.; Zhao, K. *Principles and Technology of Determination on Plant's Adaptation to Karst Environment*; Science Press: Beijing, China, 2018.
2. Wu, Y.Y.; Xu, W.X. Effect of plant growth regulators on the growth of *Orychophragmus violaceus* plantlets in vitro. *Planta Med.* **2011**, *77*, 1292–1293. [CrossRef]
3. Wang, R.; Wu, Y.Y.; Hang, H.T.; Liu, Y.; Xie, T.X.; Zhang, K.Y.; Li, H.T. *Orychophragmus violaceus* L., a marginal land-based plant for biodiesel feedstock: Heterogeneous catalysis, fuel properties, and potential. *Energy Convers. Manag.* **2014**, *84*, 497–502. [CrossRef]
4. Xing, D.k.; Chen, X.L.; Wu, Y.Y.; Xu, X.J.; Chen, Q.; Li, L.; Zhang, C. Rapid prediction of the re-watering time point of *Orychophragmus violaceus* L. based on the online monitoring of electrophysiological indexes. *Sci. Hortic.* **2019**, *256*, 108642. [CrossRef]
5. Lu, Y.; Wu, Y.Y.; Zhang, K.Y. Dose bicarbonate affect the nitrate utilization and photosynthesis of *Orychophragmus violaceus*? *Acta Geochim.* **2018**, *6*, 875–885. [CrossRef]
6. Bhardwaj, A.R.; Joshi, G.; Kukreja, B.; Malik, V.; Arora, P.; Pandey, R.; Shukla, R.N.; Bankar, K.G.; Katiyar-Agarwal, S.; Goel, S.; et al. Global insights into high temperature and drought stress regulated genes by RNA-Seq in economically important oilseed crop *Brassica juncea*. *BMC Plant Biol.* **2015**, *15*, 9. [CrossRef]
7. Vargas-Ortiz, E.; Ramírez-Tobias, H.M.; González-Escobar, J.L.; Gutiérrez-García, A.K.; Bojorquez-Velazquez, E.; Espitia-Rangel, E.; de la Rosa, A.P.B. Biomass, chlorophyll fluorescence, and osmoregulation traits let differentiation of wild and cultivated *Amaranthus* under water stress. *J. Photochem. Photobiol. B Biol.* **2021**, *220*, 112210–112220. [CrossRef]
8. Jagiełło-Kubiec, K.; Nowakowska, K.; Łukaszewska, A.J.; Pacholczak, A. Acclimation to ex vitro conditions in ninebark. *Agronomy* **2021**, *11*, 612. [CrossRef]
9. Das, K.; Roychoudhury, A. Reactive oxygen species (ROS) and response of antioxidants as ROS-scavengers during environmental stress in plants. *Front. Environ. Sci.* **2014**, *2*, 53. [CrossRef]
10. Xing, D.K.; Chen, X.L.; Wu, Y.Y.; Li, Z.Y.; Shanjida, K. Changes in elastic modulus, leaf tensity and leaf density during dehydration of detached leaves in two plant species of Moraceae. *Chil. J. Agric. Res.* **2021**, *81*, 434–447. [CrossRef]
11. Zhang, Z.; Huang, M.; Zhao, X.; Wu, L. Adjustments of leaf traits and whole plant leaf area for balancing water supply and demand in Robinia pseudoacacia under different precipitation conditions on the Loess Plateau. *Agric. For. Meteorol.* **2019**, *279*, 107733. [CrossRef]
12. Matschi, S.; Vasquez, M.F.; Bourgault, R.; Steinbach, P.; Chamness, J.; Kaczmar, N.; Gore, M.A.; Molina, I.; Smith, L.G. Structure-function analysis of the maize bulliform cell cuticle and its potential role in dehydration and leaf rolling. *Plant Direct* **2020**, *10*, e00282. [CrossRef]
13. Vastag, E.; Cocozza, C.; Orlović, S.; Kesić, L.; Kresoja, M.; Stojnić, S. Half-sib lines of pedunculate oak (*Quercus robur* L.) respond differently to drought through biometrical, anatomical and physiological traits. *Forests* **2020**, *11*, 153. [CrossRef]

14. García-Orellana, Y.; Ortuño, M.F.; Conejero, W.; Ruiz-Sánchez, M.C. Diurnal variations in water relations of deficit irrigated lemon trees during fruit growth period. *Span. J. Agric. Res.* **2013**, *11*, 137–145. [CrossRef]
15. Zhu, S.D.; Chen, Y.J.; Ye, Q.; He, P.C.; Liu, H.; Li, R.H.; Fu, P.L.; Jiang, G.F.; Cao, K.F. Leaf turgor loss point is correlated with drought tolerance and leaf carbon economics traits. *Tree Physiol.* **2018**, *5*, 658–663. [CrossRef]
16. Xing, D.K.; Chen, L.; Wu, Y.Y.; Janusz, J.Z. Leaf physiological impedance and elasticity modulus in *Orychophragmus violaceus* seedlings subjected to repeated osmotic stress. *Sci. Hortic.* **2021**, *276*, 109763. [CrossRef]
17. Bochicchio, A.; Vazzana, C.; Puliga, S.; Alberti, A.; Cinganelli, S.; Vernieri, P. Moisture content of the dried leaf is critical to desiccation tolerance in detached leaves of the resurrection plant *Boea hygroscopica*. *Plant Growth Regul.* **1998**, *24*, 163–170. [CrossRef]
18. Wang, Z.Q.; Huang, H.; Wang, H.; Peñuelas, J.; Sardans, J.; Niinemets, Ü.; Niklas, K.J.; Li, Y.; Xie, J.B.; Wright, I.J. Leaf water content contributes to global leaf trait relationships. *Nat. Commun.* **2021**, *13*, 5525. [CrossRef]
19. Li, Z.L. *Plant Section Technique*; Science Press: Beijing, China, 1978.
20. Xing, D.K.; Chen, X.L.; Wu, Y.Y.; Chen, Q.; Li, L.; Fu, W.G.; Shu, Y. Leaf stiffness of two *Moraceae* species based on leaf tensity determined by compressing different external gripping forces under dehydration stress. *J. Plant Interact.* **2019**, *14*, 610–616. [CrossRef]
21. Zhang, M.; Wu, Y.; Xing, D.; Zhao, K.; Yu, R. Rapid measurement of drought resistance in plants based electrophysiological properties. *Trans. ASABE* **2015**, *58*, 1441–1446. [CrossRef]
22. Xing, D.K.; Mao, R.L.; Li, Z.Y.; Wu, Y.Y.; Qin, X.J.; Fu, W.G. Leaf intracellular water transport rate based on physiological impedance: A possible role of leaf internal retained water in photosynthesis and growth of tomatoes. *Front. Plant Sci.* **2022**, *13*, 845628. [CrossRef]
23. Zhang, C.; Wu, Y.; Su, Y.; Xing, D.; Dai, Y.; Wu, Y.; Fang, L. A plant's electrical parameters indicate its physiological state: A study of intracellular water metabolism. *Plants* **2020**, *9*, 1256. [CrossRef] [PubMed]
24. Petrov, P.; Petrova, A.; Dimitrov, I.; Tashev, T.; Olsovska, K.; Brestic, M.; Misheva, S. Relationships between leaf morpho-anatomy, water status and cell membrane stability in leaves of wheat seedlings subjected to severe soil drought. *J. Agron. Crop Sci.* **2018**, *204*, 219–227. [CrossRef]
25. Vitalevna, P.O.; Dmitrievna, G.O.; Dmitrievich, K.S.; Vitalevna, K.O. Physiological Features of Red Currant Adaptation to Drought and High Air Temperatures. In *Drought-Detection and Solutions*; Ondrasek, G., Ed.; IntechOpen: London, UK, 2019; pp. 1–13.
26. Oliveira, I.; Meyer, A.; Afonso, S.; Gonçalves, B. Compared leaf anatomy and water relations of commercial and traditional *Prunus dulcis* (Mill.) cultivars under rain-fed conditions. *Sci. Hortic.* **2018**, *229* (Suppl. C), 226–232. [CrossRef]
27. Xing, D.K.; Xu, X.J.; Wu, Y.Y.; Liu, Y.J.; Wu, Y.S.; Ni, J.H.; Azeem, A. Leaf tensity: A method for rapid determination of water requirement information in *Brassica napus* L. *J. Plant Interact.* **2018**, *13*, 380–387. [CrossRef]
28. Li, Z.L.; Li, R.A. Anatomical observation of assimilating branches of nine xerophytes in Gansu. *Acta Bot. Sin.* **1981**, *23*, 181–185.
29. Luan, Z.H.; Shao, D.K.; Qi, Q.G.; Zhang, Q.C.; Gao, X.; Luan, J.E.; Lin, M.F.; Jiang, W.Q. Variation of leaf traits with altitude in *Lonicera caerulea* var. *edulis* (Caprifoliaceae) from Northeastern China. *Pak. J. Bot.* **2021**, *53*, 949–957. [CrossRef]
30. Chen, J.; Shen, Z.J.; Lu, W.Z.; Liu, X.; Wu, F.H.; Gao, G.F.; Liu, Y.L.; Wu, C.S.; Yan, C.L.; Fan, H.Q. Leaf miner-induced morphological, physiological and molecular changes in mangrove plant *Avicennia marina* (Forsk.) Vierh. *Tree Physiol.* **2017**, *37*, 82–97. [CrossRef]